ISBN 978-89-952197-7-5

Centrifuge model tests on tsunami-induced failure process of composite-type breakwater with reinforcing embankment

O. Kurihara & H. Takahashi
Geotechnical Engineering Department, Port and Airport Research Institute, MPAT, Yokosuka, Japan

ABSTRACT: Composite breakwaters were damaged by tsunamis in the Great East Japan Earthquake, and the reinforcement of composite breakwaters by embankment is considered as a countermeasure. The previous studies have shown that the reinforcement by the embankment increases the bearing capacity of the composite breakwater against the sliding and bearing failure modes, however, it is important to know the failure process of the composite breakwater in order to maintain the function of the composite breakwater even if the tsunami exceeds the bearing capacity. In this study, the failure process of the composite breakwaters with embankments by tsunami overflow was investigated by centrifuge model tests. The experiments were conducted on cases with different crushed stone and cross-sections with different heights, top widths, and shapes of the embankment with and without a step. It is suggested that the failure of the composite breakwater due to the overturning of the caisson is inhibited by increasing the particle size and weight of the crushed stone and/or the cross-sectional area and width of the embankment.

Keywords: composite-type breakwater, reinforcing embankment, tsunami overflow, failure process, centrifuge

1 INTRODUCTION

In the 2011 Great East Japan Earthquake, composite-type breakwaters were damaged by the tsunami, and reinforcing the composite-type breakwaters with an embankment has been studied as a countermeasure. The resistance of the composite-type breakwaters is examined by verifying the resistance to each failure modes of sliding and bearing capacity (OCDI, 2020). For example, Takahashi et al. (2015) and Takahashi (2021) conducted loading tests with various shapes and materials of the embankment installed on a model of the composite-type breakwater to investigate the trend of increase in the resistance against sliding and bearing capacity. In addition, Arikawa et al. (2013) stated that in wave resistance experiments, the flow over the breakwater scoured the embankment and the caisson moved significantly due to the loss of the embankment by the scour.

This study considers the case where the composite-type breakwater is destroyed by a tsunami exceeding its capacity, and it is desirable to maintain its function as much as possible rather than losing it instantly. In order to protect the harbour and hinterland after the failure of the composite-type breakwater, the top height is important as the remaining function. If the caisson falls over the mound to the seabed, the top height of the composite-type breakwater will be lowered and its function will be lost, but if the top height can be maintained even a little after the fall, the protection function of the composite-type breakwater can be fulfilled immediately after the failure. It is necessary to study the failure process of composite-type breakwaters, but there is no detailed study of the post-failure state. In this study, the failure process of a composite-type breakwater with an embankment by tsunami overflow was investigated by centrifuge model tests, and the method of the experiment is presented in detail.

2 EXPERIMENTAL CONDITIONS

In this study, experiments were carried out in a centrifuge field which can reproduce the real-scale stresses and water pressures in the ground (Takahashi et al., 2019). In each case where the shape and material of an embankment were changed, a water level difference was generated in front of and behind a composite-type breakwater, and the breakwater was failed. This study mainly focused on the overturning mode that leads to catastrophic failure.

The cross-sectional view of the experiment is shown in Fig. 1 and the model of the composite-type breakwater is shown in Fig. 2. The size of the model is 1/50 of the real scale and the centrifugal acceleration is 50 *g*. The inner dimensions of the container for the model part are 140 cm wide, 60 cm deep and 8 cm long and the real scale equivalent at 50 *g* is 70 m wide, 30 m deep and 4 m long. Behind the model part there is a drainage tank. Friction between the caisson or the ground and the container wall was reduced by pasting grease-coated membranes and sponge tape. The foundation ground is dense sand with D_r = 90% and has little effect on the deformation of the mound and the embankment in the experiments. The water level was maintained by pouring

Table 1. Experimental conditions and results.

(a) The cases of different materials of the embankment

Case	Conditions							Results			
	Embankment									Overturned caisson	
	Height	Top width	Step width	Sectional area	Stone size	w**	v***	Overflow	Scour	Height****	Position
G1-B-FN	4/12 *H*	4/12 *H*	—	52.9 m^2	2–3mm	9.2 m	18.6 m^2	*	*	33% IV	C
G1-B	4/12 *H*	4/12 *H*	—	52.9 m^2	5–7mm	9.2 m	18.6 m^2	✓	✓	19% IV	F
G1-B-CS	4/12 *H*	4/12 *H*	—	52.9 m^2	10mm	9.2 m	18.6 m^2	✓		106% I	A

(b) The cases of different shapes of the embankment

Case	Conditions							Results			
	Embankment									Overturned caisson	
	Height	Top width	Step width	Sectional area	Stone size	w**	v***	Overflow	Scour	Height****	Position
G0	—	—	—	0 m^2	5–7mm	2.3 m	0 m^2			30% IV	F
G0-STG	—	—	1.75 *H*	80.5 m^2	5–7mm	18.4 m	0 m^2			60% III	C
G1-B	4/12 *H*	4/12 *H*	—	52.9 m^2	5–7mm	9.2 m	18.6 m^2	✓	✓	19% IV	F
G1-B-STG3	4/12 *H*	4/12 *H*	0.75 *H*	87.6 m^2	5–7mm	16.1 m	18.6 m^2	*	*	51% III	C
G1-M2	5/12 *H*	5/12 *H*	—	75.9 m^2	5–7mm	11.6 m	29.6 m^2	*	*	19% IV	F
G1-M2-STG	5/12 *H*	5/12 *H*	0.5 *H*	98.6 m^2	5–7mm	16.1 m	29.6 m^2	✓	✓	86% II	B
G1-TW	6/12 *H*	6/12 *H*	—	99.8 m^2	5–7mm	13.8 m	42.3 m^2	✓	✓	66% III	C
G1-M	7/12 *H*	7/12 *H*	—	126.0 m^2	5–7mm	16.1 m	57.2 m^2	✓	✓	104% I	A
G1-TW2	6/12 *H*	12/12 *H*	—	144.0 m^2	5–7mm	18.4 m	63.5 m^2	✓	✓	101% I	S

* The caisson was overturned because of the discharge of crushed stones from the embankment due to seepage flow rather than a slight overflow.
** w is the width of the embankment at the mound top height.
*** v is the cross-sectional area of the embankment above the mound top height.
**** I: 90–100%, II: 70–90%, III: 40–70%, IV: 0–40%

water from the water tank at the top of the container to the front of the composite-type breakwater and draining it through the drainage hole at the back of the embankment in order to generate a difference in water level modelled as a tsunami. The composite-type breakwater movement were filmed using a high-speed camera installed in front of the model container.

Examples of the water level rises from the initial water level and their water level difference between the front and the back of the caisson are shown in Fig. 3. This figure shows the measurements made by the water pressure gauges in Case G1-TW2, in which the caisson was almost stable. The time is shown in model scale, and the water level rise and the water level difference are shown in real scale. The water level rise at the front of the caisson was 0.8 s, and the water level rise at the back of the caisson was 1.2 s before the steady state was reached. Since there is a difference in the time taken for the water level to become constant at the front and back of the caisson, the difference in water level between the front and back of the caisson is 9m on the real scale for 0.5–0.8 seconds and then becomes constant at 7m. It remains constant for about 8 seconds. When the water level difference is 9.2m, the bearing capacity ratio is 0.98.

Photographs of the caisson model and the crushed stone used as materials for the mound and embankment are shown in Fig. 4. The weight of the caisson model was adjusted by filling an assembled acrylic box with sand and lead balls. The average weight of each crushed stone

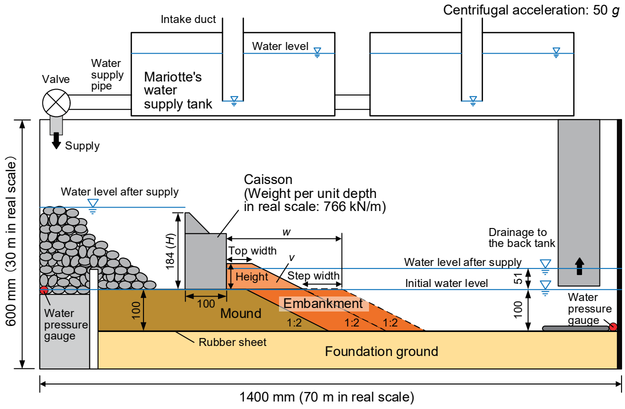

Fig. 1. Experimental cross-section.

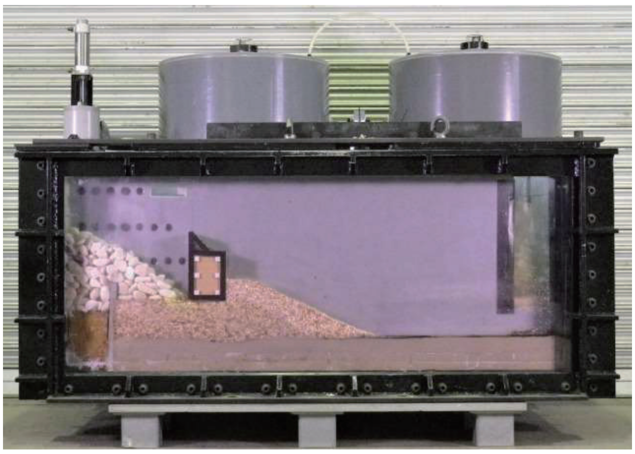

Fig. 2. Experimental model and container.

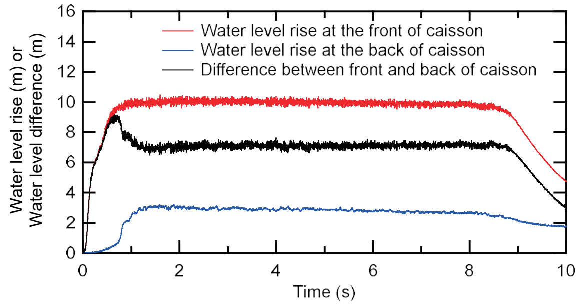

Fig. 3. Water level rise and difference in case G1-TW2.

was 0.106 g (13 kg) for 2–3 mm (10–15 cm) crushed stone, 0.14 g (18 kg) for 5–7 mm (25–35 cm) crushed stone, and 2.34 g (293 kg) for 10 mm (50 cm) crushed stone. Note that the values in parentheses are actual scales. All sizes of crushed stone are angular in shape.

Table 1 (a) shows the experimental conditions for the cases of different materials of the embankment. In these cases, the height and the top width of the embankment are 1/3 *H*, where the height of the front of the caisson including the parapet is *H*. The materials of the mound and the embankment are 2–3 mm, 5–7 mm and 10 mm crushed stone.

Table 1(b) shows the experimental conditions for the cases with different shapes of the embankment. In these cases, the height and the top width of the embankment were changed, and the width of the embankment at the same height as the top of the mound was changed by adding a small step in the middle of the embankment slope (*-STG) to prevent the overturned caisson from sliding off the mound. G0 is the case without the embankment, and G0-STG is the case with a mound extension width. G1-TW2 is the case that the top width of the embankment is twice as wide as G1-TW. In all these cases, 5–7 mm crushed stone was used for the mound and embankment.

3 EXPERIMENTAL RESULTS

3.1 Experiments with different materials for the embankment

The snapshots of the experiments are shown in Fig. 5. The yellow dashed line shows the position of the caisson and the embankment before the experiment, and the red dashed line shows the position of the caisson after the experiment. G1-B-FN, G1-B, and G1-B-CS are made of 2–3 mm, 5–7 mm, and 10 mm crushed stone, respectively. The height and the top width of the embankment is 1/3 *H* in these cases.

In G1-B-FN, seepage flow started to wash out the crushed stones on the embankment slope before overflowing, and the caisson overturned without scouring after slight overflowing. In G1-B, the embankment slope scoured after overflowing, and the caisson overturned. After the overturning, the caisson in G1-B-FN slid down to just above the foundation ground level, and the caisson in G1-B slid down to the foundation ground level. In G1-B-CS, relatively large seepage flow occurred on the embankment slope when the difference of the water level between the front and the back of the composite-type breakwater started to increase, but the embankment slope was not washed out. The water level difference caused the caisson to tilt gradually, and a few crushed stones on the embankment slope were rolled over, but the embankment was not scoured by the overflow. Even after the increase in the tilt of the caisson was stopped, the overflow continued due to the water level difference, but the embankment was not scoured, and the caisson did not overturn. It was found that the larger the particle size and weight of the crushed stone are, the less the crushed stones were washed away by seepage and the less the embankment was scoured by overflow.

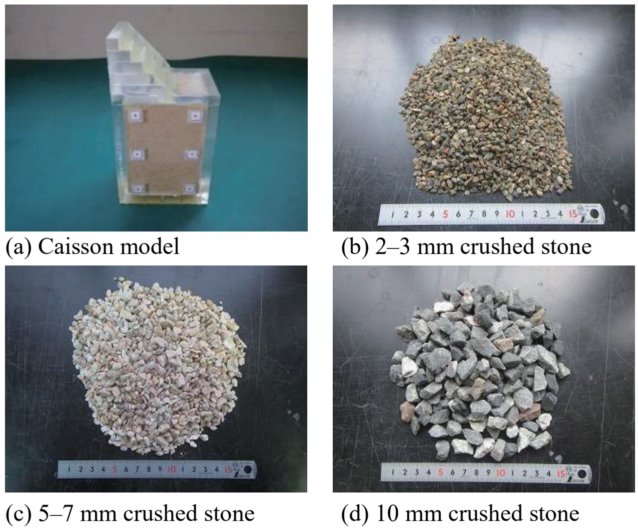

Fig. 4. Caisson model and embankment materials.

3.2 Experiments with different shapes of embankment

On the left side of Fig. 5, snapshots of G1-B, G1-M2, G1-TW and G1-M are shown as cases where the height and the top width of the embankment are increased simultaneously. It can be seen that the overturned caisson slides down to the foundation ground level until the embankment is increased to a certain size, and the caisson loses its height at once when it overturns. The G0-STG, G1-B-STG3 and G1-M2-STG shown on the right side of Fig.5 are the cases with a small step in the middle of the embankment. If the width of the small step is long enough, the overturned caisson does not slide down to the foundation and the height of the caisson can be maintained to some extent after the overturn.

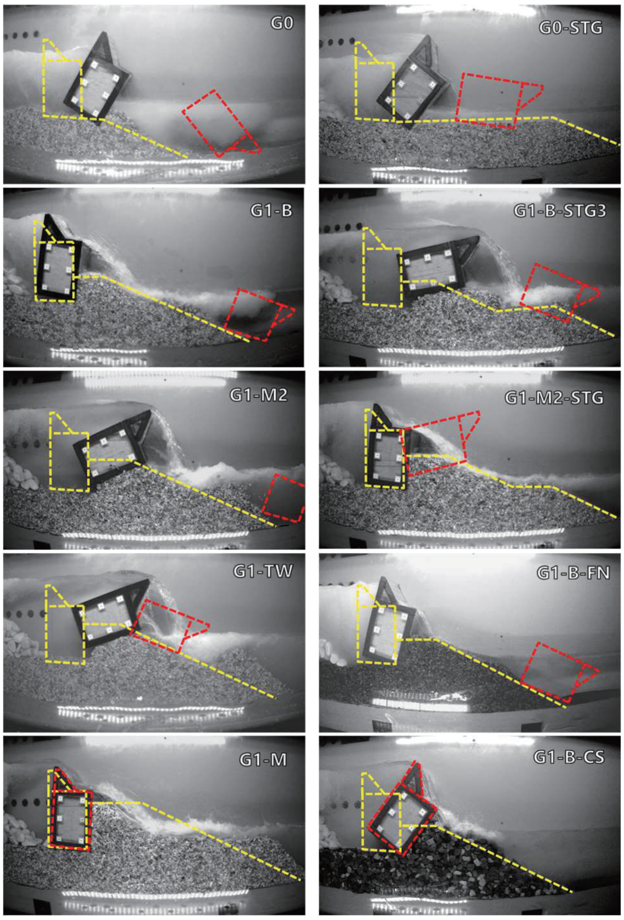

Fig. 5. Snapshots taken by the high-speed camera.

3.3 Summary of experimental results

The results of the experiment are summarised on the right side of Table 1. In G0 and G0-STG, the caisson overturned due to the difference in water levels before overflowing and scouring. In G1-B-STG3 and G1-M2, the caisson overturned due to the discharge of crushed stone from the embankment by seepage flow rather than slight overflow. In other cases, the caissons overturned after overflowing and scouring.

The height and position of the caisson after overturning were classified by the indices shown in Fig. 6. The cross-sectional area *v* of the embankment at the height above the mound top and the width *w* of the embankment at the height of the mound top are defined in Fig. 1. As shown in Fig. 6, the caisson in each case overturns the embankment and falls to the foundation ground. In this experiment, it was found that the caisson could be prevented from sliding down to the foundation ground by increasing the width *w* of the embankment with a small step, even though the caisson fell to the foundation ground in the case without a small step. On the other hand, when the cross-sectional area *v* was increased, the caisson could be stopped at the stage before it climbed over the embankment.

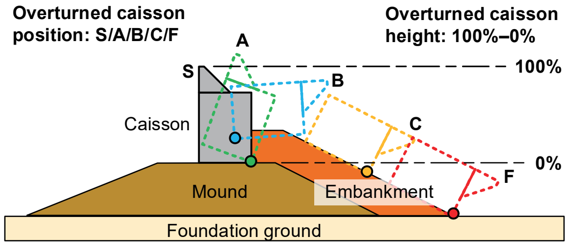

Fig. 6. Position and height of overturned caisson.

4 CONCLUSIONS

The results obtained in this study are summarized as follows.

1) Centrifuge model tests were carried out on composite-type breakwaters with a basic shape of the embankment and three different types of crushed stones for the mound and the embankment, and the caisson was overturned. The results showed that the failure of the composite-type breakwater progressed differently depending on the size and weight of the crushed stones of the embankment.
2) Centrifuge model tests were carried out on composite-type breakwaters with several shapes of embankment with different heights, widths and small steps of the embankment, and the caisson was overturned. It is shown that the size in the cross-sectional area *v* of the embankment above the mound top and the width *w* of the embankment at the mound top height affects the position and height of the caisson after overturning.

REFERENCES

Arikawa, T., Sato, M., Shimosako, K., Tomita, T., Yeom G., and Niwa, T. 2013. Failure Mechanism and Resiliency of Breakwaters under Tsunami. *Technical Note of the Port and Airport Research Institute*, 1269, 37p. (in Japanese)

Takahashi, H. 2021. Stability of composite-type breakwaters reinforced by rubble embankment. *Soils and Foundations*, *61*(2), 318–334.

Takahashi, H., Fujii, N., Morikawa, Y., and Takano, D. 2019. Development of hydro-geotechnical centrifuge PARI Mark II-R. *Technical Note of the Port and Airport Re-search Institute*, 1353, 27p.

Takahashi, H., Sassa, S., Morikawa, Y., Watabe, Y., and Takano, D. 2015. Stability of caisson-type breakwater's mound and reinforcing embankment against tsunami. *Report of the Port and Airport Research Institute*, *54*(2), 21–50. (in Japanese)

The Overseas Coastal Area Development Institute of Japan (OCDI). 2020. Technical standards and commentaries for port and harbour facilities in Japan.